DELIVERABLE D3.2
1D/2D DFN MODELS OF BOREHOLE FRACTURES AND HYDRAULIC CIRCULATION SIMULATIONS

WP3: UPSCALING OF THERMAL POWER PRODUCTION AND OPTIMIZED OPERATION OF EGS PLANTS

Contractual delivery date:	M12
Actual delivery date:	M12

PROJECT INFORMATION

Grant Agreement n°	792037
Dates	1st May 2018 – 31 October 2021

DOCUMENT INFORMATION

Version	VF	**Dissemination level**	PU
Editor	TUDa		
Other authors	ESG, ULS and GEOT		

DOCUMENT APPROVAL

Name	Position in project	Organisation	Date	Visa
ALBERT GENTER ELEONORE DALMAIS	Project Coordinator	ES GEOTHERMIE	25/04/2019	OK
ELEONORE DALMAIS	WP Leader	ES GEOTHERMIE	24/04/2019	OK
MARGAUX MAROT	Project Manager Officer	AYMING	23/04/2019	OK
JOHN REINECKER	Internal Reviewer	GEOT	15/04/2019	OK

DOCUMENT HISTORY

Version	Date	Modifications	Authors
V1	14/04/2019	ToC	AFSHARI / TUDa
V2	15/04/2019	Internal review	REINECKER / GEOT
V3	23/04/2019	Internal review	MAROT / AYMING
V4	24/04/2019	Modification	AFSHARI / TUDa
VF	25/04/2019	Final approval	GENTER / ESG

CONTENT

1 EXECUTIVE SUMMARY

1.1 DESCRIPTION OF THE DELIVERABLE CONTENT AND PURPOSE

Enhanced Geothermal Systems (EGSs) aim to circulate a fluid (e.g. water) between the injection and production wells in a reservoir system to exploit the heat stored in the earth's crust. The commercial development of EGS plants requires sufficient fluid flow rates with high temperatures. Matrix permeability of crystalline host rocks is generally insufficient to serve the required high flow rates. Therefore, hydraulically active fracture networks are essential to support effective fluid flow pathways. The reservoir productivity/injectivity index of EGS reservoirs needs to be increased and maintained by thermal, hydraulic and chemical stimulations. Hydraulic stimulation typically results in significant permeability enhancement (two to three orders of magnitude) such as Soultz-sous-Forêts EGS (e.g.Evans et al. 2005). On the other hand, THMC stimulation operations may be accompanied by micro-seismicity and sometimes felt earthquakes, such as observed during the stimulation of the Basel EGS project in Switzerland, which led to project curtailment (Häring et al. 2008).

The processes involved in THMC stimulation and forced circulation experiments are complex and well-understood, including thermo-hydromechanically coupled processes. Therefore, the research on optimizing the operational parameters to improve the connectivity within the fracture network and enhance the permeability, while reducing the risk of induced-seismicity is currently ongoing. This requires a comprehensive characterization of the rock mass resulting in representative geological models of the fractured rocks to simulate the relevant thermo-hydromechanical processes. Such geological models must include information on the geological features such as fractures and faults from small to large scales.

Geophysical techniques from surface are limited in resolution when dealing with great depth and reflection seismic technology is difficult to interpret in crystalline basement rocks, because potential reflectors are inherently not well defined. Well logging techniques (e.g. acoustic televiewer logs) and core samples are the typical sources of information on the fracture network in the reservoir. However, deterministic reconstruction of 3D structural model of the fracture network from 1D datasets (both from cores and image logs) is a not resolved yet (Afshari Moein et al. 2019). Borehole data provide the statistical parameters of fractures intersected by the wellbore including the spatial distribution and orientation of fractures. These parameters are necessary to generate stochastic realizations, known as Discrete Fracture Network (DFN) models. These DFN models must be constrained with further information from induced seismicity patterns, in situ stress and hydraulic data.

In this research, the aim is to create a DFN model of the Soultz-sous-Forêts Geothermal Site in France that matches with the hydraulic circulation experiments. However, prior to creating a 3D fluid flow model, there should be: 1) a fundamental understanding of the fracture network characteristics in deep geothermal systems and 2) clarification of the any depth dependencies of the fracture network characteristics versus depth. At the moment, the main focus of the research is largely on these two major subjects and the hydraulic circulation model is not fully developed yet and will be included in future developments of this work in near future. However, the methodology to generate hydraulic circulation model is currently developed and presented in

the chapter 2.6. This methodology will be further implemented to hydraulic circulation experiments in Soultz-sous-Forêts.

1.2 BRIEF DESCRIPTION OF THE STATE OF THE ART AND THE INNOVATION BREAKTHROUGHS

The global tendency to curtail the CO_2 emissions requires a reduction of fossil fuel consumption that is achieved by developing renewable resources such as geothermal energy. The huge amount of heat stored in the earth's crust, that is not presently exploited (e.g. Tester et al. 2006), demands extensive efforts to develop the necessary technologies for widespread heat extraction and electricity production. Current operational geothermal plants are limited to certain geological settings where ideal temperatures are found in high permeability host rocks. Enhanced Geothermal Systems (EGS) aim at creating a reservoir at high temperature depths, typically between 2-5 km depth, to circulate fluids (e.g. water) between injection and production boreholes, where the fluid flow occurs mainly through the fracture network (Genter et al. 2010). This is often achieved by enhancing the permeability by massive fluid injections in target zones, referred as hydraulic stimulation. It has been observed that hydraulic stimulation typically results in increases the permeability 2-3 orders of magnitude at site scale (Evans et al. 2012; Häring et al. 2008). Furthermore, hydraulic circulations are also necessary to maintain the permeability in the lifetime of a reservoir.

The thermo-hydromechanically (THM) coupled processes activated during THMC stimulation are very complex. Nevertheless, the borehole data and geophysical observations suggest that reactivation of pre-existing fracture planes in shear due to pore pressure increase (Evans 2005; Evans et al. 2005). THMC stimulation may be accompanied with induced seismicity, that may result in damaging events and lead to project suspension like in Basel (Häring et al. 2008) and St. Gallen geothermal projects in Switzerland (Edwards et al. 2015; Moeck et al. 2015). Therefore, the efforts should focus on optimizing the stimulation scenarios to enhance the permeability while keeping the seismicity in safe levels. This is achieved by developing numerical models that can simulate the associated physical processes in complex structural geometries of the fractured rocks. Not only hydraulic stimulation, but also any hydraulic circulation experiments also triggers (THM) coupled processes in fractured rock mass.

Fracture network geometry is believed to largely control not only the fluid flow, geomechanical interactions and heat exchange between the fluid and the host rock. Therefore, the knowledge on the natural fracture network is a critical element fo designing and evaluating stimulation and circulation scenarios in deep geothermal systems. The characterization of deep geothermal reservoirs is a challenging task. Surface outcrops of geothermal reservoirs are often not available, and if available a correlation of the derived characteristics or parameter to reservoir depths is not straightforward. Geophysical techniques from surface are limited in resolution when dealing with great depth and reflection seismic technology is difficult to interpret in crystalline basement rocks, because potential reflectors are inherently not well defined. More relevant data can be acquired by wellbore geophysical logging. Valley and Evans (2015) provide a summary of the state-of-the-art in reservoir characterization from borehole measurements and identify gaps and research needs.

The initial source of information about the natural fractures within EGS reservoirs stems from borehole images (e.g. ultrasonic and resistivity image logs) and core samples, if available. However, continuous coring from deep boreholes are very costly and very rare, limiting the fracture data to borehole imagery. These logs identify the position and orientation of fractures along the borehole. Similar information may be acquired from cores, too. However, fracture network characterization is challenging at early project stages, especially when data from only a single exploration well penetrating the target reservoir may be available.

Deterministic reconstruction of 3D fracture network from borehole images is a challenging task. Thus, stochastic realizations known as Discrete Fracture Network (DFN) models are implemented and conditioned by statistical parameters observed from the wellbore fractures including the spatial distribution and orientation of fractures. DFN models may also be constrained with other sources of information including hydraulic data (Somogyvári et al. 2017), in situ stress perturbations observed in image logs (Afshari Moein et al. 2018b) and induced seismicity patterns (Afshari Moein et al. 2018c). DFN models are widely used to model the hydromechanical response of fractured rock mass in many subsurface engineering applications (Lei et al. 2017).

Among various DFN models presented in literature, fractal DFNs have gained a large attention, since they allow generating multiscale fracture patterns following similar statistics at different scales. An extensive amount of field observations also supports the hypothesis that fracture network attributes such as spatial patterns, length distribution, spacing and aperture follow power-law statistics (e.g. Allegre et al. 1982; Barton and Zoback 1992; Boadu and Long 1994; Bonnet et al. 2001; Lei and Wang 2016; Tezuka and Watanabe 2000; Torabi and Berg 2011). In order to parameterize fractal DFN models, it is crucial to reliably estimate the scaling exponent (i.e. fractal dimension) of different attributes particularly spatial distribution.

Proper application of fractal DFN models at the scale of a geothermal reservoir demands adequate understanding on the potential depth dependence of spatial patterns in earth's crust. Such a depth-dependence may be implemented to anticipate deeper reservoir conditions from shallower datasets. Ledésert et al. (1993) reported a global increase of the fractal dimension with depth by analyzing the facture data from core samples in EPS1 borehole drilled into basement rocks in Soultz-sous-Forêts geothermal site. However, the validity of such a trend is questionable, because they implemented the box-counting technique to obtain the fractal dimension of fracture patterns which is likely influenced by inherent bias originating from finite size effects. This influence has been confirmed by studies on spatial distribution of fractures in synthetic data, deep boreholes and outcrops in Hornelen Basin (Afshari Moein et al. 2019; Bour et al. 2002) and reliable fractal dimensions (correlation dimension) may be estimated using two-point correlation function. Both box-counting and two-point correlation functions are illustrated in the methodologies.

This deliverable aims to answer the following detailed questions with an exceptional collection of fracture datasets from seven deep boreholes drilled into crystalline basement rocks: 1) Do the fracture patterns in all wells follow fractal statistics? 2) What is the effect of fracture data source (i.e. core samples or image logs) on the scaling exponents of fractures, if the fracture patterns are fractal? 3) How does the scaling exponent of fracture patterns change versus depth, if the fracture patterns are fractal? 4) How does the fracture density change as a function of depth? 5)

How to implement the findings of this research into practical applications and hydraulic circulation models?
This deliverable starts with a brief overview on the methodologies implemented to characterize the fractures in 1D borehole data including box-counting and two-point correlation function. Then, two-point correlation method is implemented to study the scaling properties of fracture datasets from image logs from Basel-1 (borehole drilled into the Basel geothermal project in Switzerland), GPK1, GPK2, GPK3, GPK4 (boreholes drilled into the Soultz-sous-Forêts geothermal project in France), RH-15 (borehole drilled into the Rosemanowes geothermal project in UK) as well as the core samples from EPS1 borehole at the Soultz-sous-Forêts site. Then, the depth-dependence of scaling properties of fracture patterns is further investigated. The detailed analyses of the fracture datasets will be integrated to set up synthetic fractal DFNs to be implemented in simulating the fluid flow model of the hydraulic circulation models of the Soultz-sous-Forêts geothermal site.

1.3 CORRECTIVE ACTION (IF RELEVANT)

n/a

1.4 IPR ISSUES (IF RELEVANT)

n/a

2 DELIVERABLE REPORT

2.1 METHODOLOGY TO CHARACTERIZE THE SCALING OF 1D FRACTURE PATTERNS

Fractal geometry has been widely used to characterize the scaling properties of fracture patterns in geological media (e.g. Bonnet et al. 2001; Torabi and Berg 2011). Since data from a deep geothermal reservoir is typically 1D fracture datasets including the location and orientation of fractures intersecting the borehole, it is necessary to characterize the available data statistically to gain insights on the geometrical properties of fracture network. The spatial distribution of 1D fracture patterns may be characterized by a scaling exponent, known as fractal dimension *D*, which is a measure of clustering degree. The fractal dimension of 1D fractal patterns is a number between 0 and 1, of which lower values indicate higher degree of clustering and a value close to 1 indicates a more homogeneous distribution. Values for fractal dimension for of 2D fractal fracture patterns are between 1 and 2, for 3D fractal fracture pattern between 2 and 3.
A detailed overview of the methodologies to estimate 1D fractal dimensions are presented by Afshari Moein et al. (2019). However, in the following we briefly illustrate the two main widely used methodologies in literature and discuss their implications for 1D borehole datasets from deep borehole. Note that all methodologies must deliver the same scaling exponent for a given fractal pattern.

2.1.1 Box-counting technique

In Box-counting technique, continuous equal-sized rulers (t) are applied to count the number of rulers $N(t)$ required to cover the entire fracture pattern. The process starts with a ruler as long as the domain length (here the scanline or borehole interval length) and progressively decreasing the ruler size to the fractions of the domain length. In a fractal distribution, $N_b(t)$ scales with the ruler size as in equation 1, where D_b represents the box-counting fractal dimension.

$$N_b(t) \sim t^{-D_b} \quad (1)$$

The box-dimension D_b is computed by measuring the local slope of $N_b(t)$ as a function ruler length in a log-log domain. This technique has been applied to characterize the scaling of 1D and 2D fracture patterns (e.g. Berkowitz and Hadad 1997; Chilès 1988; Ehlen 2000; La Pointe 1988; Moein et al. 2016; Odling 1992).
Box-counting technique is also known as Cantor's Dust method in which $\frac{Nb(t)}{N}$ scales with the ruler length t, with an exponent of $1-D_b$, where N is the total number of rulers of length t (e.g. Ledésert et al. 1993; Moein et al. 2016; Velde et al. 1990). According to the extensive analysis of the synthetic fracture patterns of known fractal dimension generated using the Multiplicative Cascade process (Darcel et al. 2003a), box-counting technique did not deliver reliable estimates of the fractal dimension (Afshari Moein et al. 2019). The plot of $N_b(t)$ in a log-log space may be linear for a limited range of scales, imposing a large amount of bias on estimating the fractal dimension. This observation is also valid for 2D fracture networks. Bour et al. (2002) implemented the so-called box-counting technique to perform a fractal analysis of an outcrop in the Hornelen

Basin, Norway, without being able to estimate a fractal dimension and concluded that this technique is strongly affected by finite size effects.
The box-counting technique briefly presented to clarify the comparison with previous studies despite being used in this deliverable. However, Ledésert et al. (1993) have applied this method to extract the depth-dependent scaling of fractures in EPS1 well. In contrast to Ledésert et al. (1993), here we apply the two-point correlation function method to perform a detailed fractal analysis.

2.1.2 Two-point correlation function

The two-point correlation function or correlation integral (referred as correlation function later on) measures the probability of finding pair of fractures separated by a given center-to-center distance (Hentschel and Procaccia 1983). Correlation function may be applied to characterize the clustering of fracture centers in 1D, 2D and 3D fracture networks through equation 2,

$$C(r) = \frac{2}{N(N-1)} N_p(r) \sim r^D \qquad (2)$$

where, N is the total number of fractures, N_p is the number of pairs of fractures whose center-to-center distance is less than *r* and the total number of pairs of fractures is $\frac{N(N-1)}{2}$.
It has been confirmed that the correlation function method is the only technique that permits a reliable and stable estimation of fractal dimension over a large range of scales for 1D and 2D datasets (Afshari Moein et al. 2019; Bour et al. 2002). Note that correlation function has also been applied to characterize the scaling properties of microearthquake hypocenters (Afshari Moein et al. 2018c; Hirata et al. 1987).

2.2 1D BOREHOLE DATASETS FROM GEOTHERMAL SYSTEMS

The information on the fracture network in geothermal reservoirs is limited to the borehole image logs and cores samples, if available. Here, we analyze the spatial distribution of fractures in seven deep boreholes drilled into the crystalline basement rocks, one of which stems from core samples (EPS1) and the rest originate from image logs. The resolution of borehole image logs limits the identification and mapping of thin fractures (Genter et al. 1997). Generally, borehole images fail to detect the sealed fractures thinner than 3 mm, because of the resolution limits. However, image logs provide statistical properties such as spatial organization and fracture families that likely
Control the fluid flow within the fractured rock. However, this study tries to extract the depth-dependent scaling properties of the fracture patterns in deep boreholes both from image logs and core samples.
Thus, a unique collection of 1D fracture datasets from seven deep wells are available:
1) Basel-1 borehole drilled at the Basel geothermal project located near Basel in Switzerland,
2) EPS1, GPK1, GPK2, GPK3 and GPK4 wells drilled at the Soultz-sous-Forêts geothermal project in France,
3) RH-15 well drilled at the Rosemanowes geothermal site in the UK.

The datasets include information on the location and orientation of fractures along the boreholes. Additional information such as the aperture, fracture fillings etc. is also available for the fractures from EPS1, where 810 m of continuous core samples exists. The depth of fractures in the borehole logs has been converted from measured depth (MD) to true vertical depth (TVD) below the ground.
Table 1 presents an overview of the available fracture datasets in this analysis, including the interval of crystalline basement at each well, the source of fracture datasets (i.e. cores or image logs) and the number of identified natural fractures. The GPK1 and RH-15 wells have the least number of fractures among the available wells. This may be due to the poor quality of the image logs or operational problems during the logging period.
A brief introduction on the project, the geological setting and the available wells in each reservoir is provided in the following subchapters.

Table 1. The relevant information of the fracture datasets from seven deep boreholes drilled into the crystalline basement in three geothermal sites (Basel, Soultz-sous-Forêts and Rosemanowes)

Well	Basement Interval TVD [m]	Source of information	Number of fractures
Basel-1	2600-5000 m	Image Log	1164
EPS1	1417-2227 m	Cores	2997
GPK1	1376-3600 m	Image Log	593
GPK2	1420-3800 m	Image Log	1785
GPK3	1420-5000 m	Image Log	1926
GPK4	1420-5000 m	Image Log	2115
RH-15	2200-2780 m	Image Log	323

2.2.1 Basel Geothermal Site

The Basel geothermal project aimed to develop an EGS for electricity production and district heating in the city of Basel, Switzerland. Basel is located at the southern end of the Upper Rhine Graben known as a Cenozoic rift system. Basel-1 well was drilled to a depth of 5 km penetrating 2.4 km of Quaternary, Tertiary, Mesozoic and Permian sediments and 2.6 km of magmatic rocks (Häring et al., 2008). The magmatic rock types include mainly granitoid rocks (>99%), aplite and lamprophyre (Kaeser, Kalt, & Borel, 2007). The top section of the basement is highly altered since it was exposed at the surface prior the deposition of the Permian sediments. Basel-1 well is approximately vertical and the borehole was imaged by Ultrasonic Borehole Imager (UBI) before installing the casing. Ziegler et al. (2015) performed a comprehensive analysis of the fracture data from the UBI logs and identified 1164 natural fractures (Table 1). They also analyzed the orientation of fractures by cluster analysis and found six potential fracture families/sets. In this study, we use the same dataset. Figure 1 present the isodensity (lower-hemisphere and equal angle) projection of poles of fractures observed in the Basel-1 well.

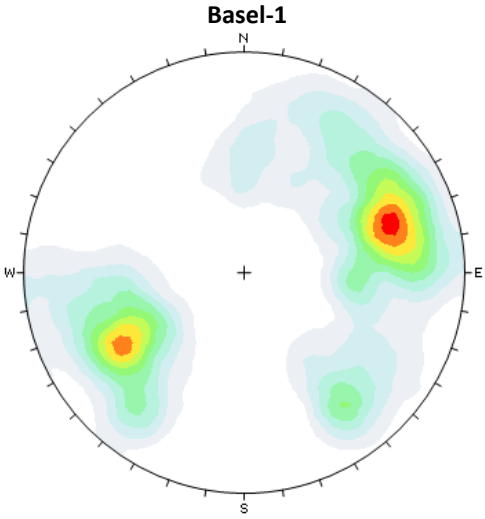

Figure 1. Isodensity (lower-hemisphere and equal angle) projection of poles of all fractures observed on image logs in the Basel-1 well drilled into Basel geothermal site.

2.2.2 Soultz-sous-Forêts Geothermal Site

The Soultz-sous-Forêts geothermal site, also known as European EGS project, is located near the western border fault of the Upper Rhine Graben in France. Since the start of the project, five boreholes have been drilled to develop a heat exchanger within the crystalline basement that are covered by 1.4 km of Mesozoic and Cenozoic sediments. Two exploratory wells (EPS1 and GPK1) and three exploitation wells (GPK2, GPK3 and GPK4) were drilled to investigate the research questions in EGS technology.

The granitic rock at Soultz-sous-Forêts is a Hercynian monzogranite with various levels of hydrothermal alteration (Dezayes et al. 2010; Sausse et al. 2008). Two main granitic rocks are commonly found in Soultz: 1) Mega K-Feldspar monzogranite that is typically found between 1420 to 4700 m depth, 2) fined-grained two-mica granite from 4.7 km to 5km (Dezayes et al. 2005).

The fracture datasets from cores and image logs from EPS1, GPK1 and GPK2 were presented in previous research projects (Genter et al. 1997; Genter and Traineau 1992; Genter et al. 1996). Valley (2007) also analyzed the borehole images from GPK3 and GPK4 and defined seven fracture sets in two wells. Here, we used the same fracture datasets. Figures 2 and 3 present the isodensity (lower-hemisphere and equal angle) projection of poles of fractures observed in GPK1, GPK2, GPK3 and GPK4 from image logs and EPS1 from core samples.

2.2.3 Rosemanowes Geothermal Site

The UK Hot-Dry-Rock (HDR) project was located in Rosemanowes in Cornwall. Three deep boreholes RH-11, RH-12 and RH-15 were drilled into the Carnmellis granite batholith. The fracture data from RH-12 is not available and RH-12 does not include sufficient fractures to perform a fractal analysis. Furthermore, the orientation of all fracture in the available dataset seems to be incomplete. RH-15 contains 323 fractures and the corresponding depth is measure

depth. Since the trajectory data was not available at the time of this analysis, we only performed the calculations using measured depth (MD).

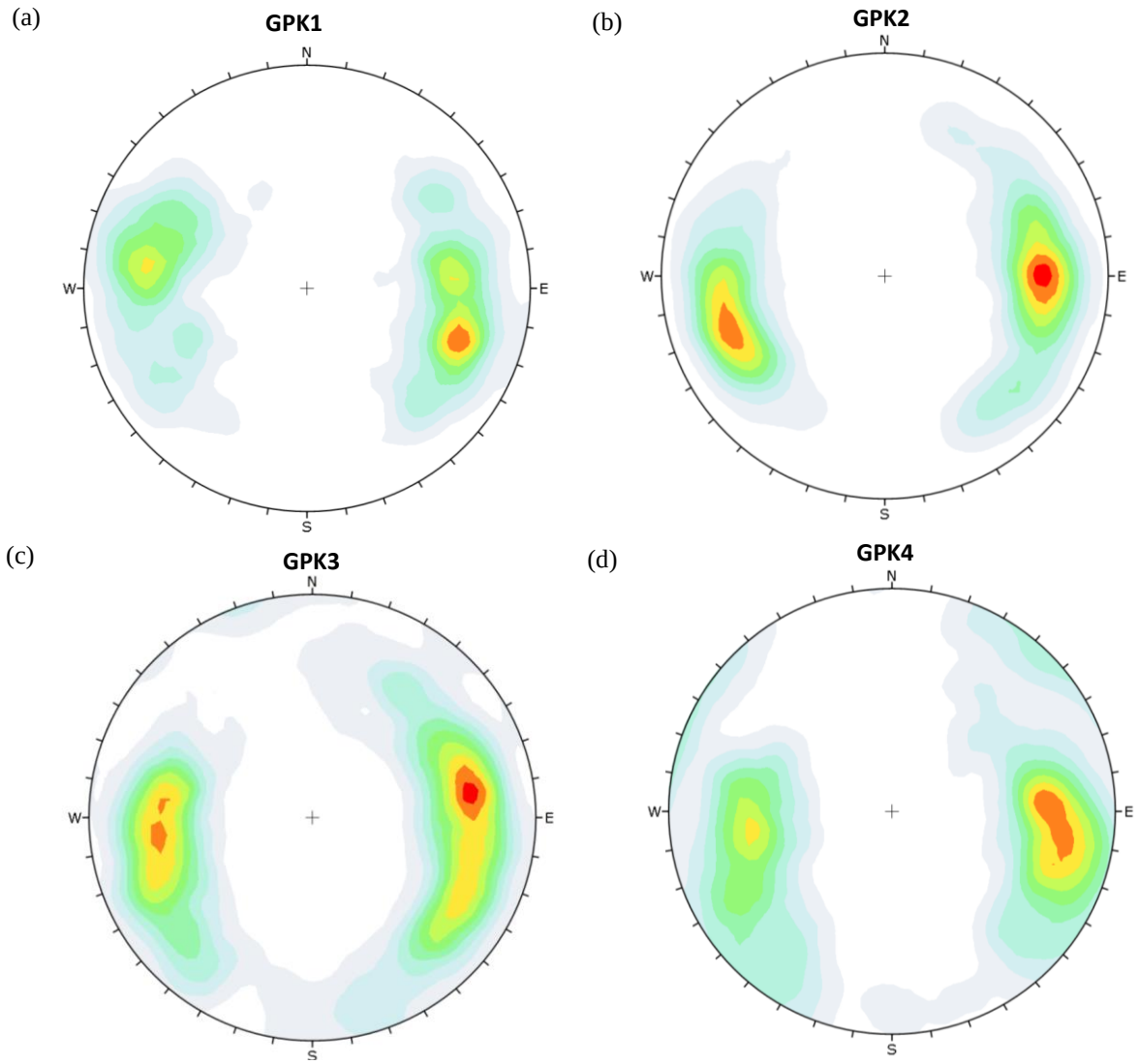

Figure 2. Isodensity (lower-hemisphere and equal angle) projection of poles of fractures observed on image logs in the wells drilled into Soultz-sous-Forêts geothermal site (a) GPK1 (b) GPK2 (c) GPK3 and (d) GPK4.

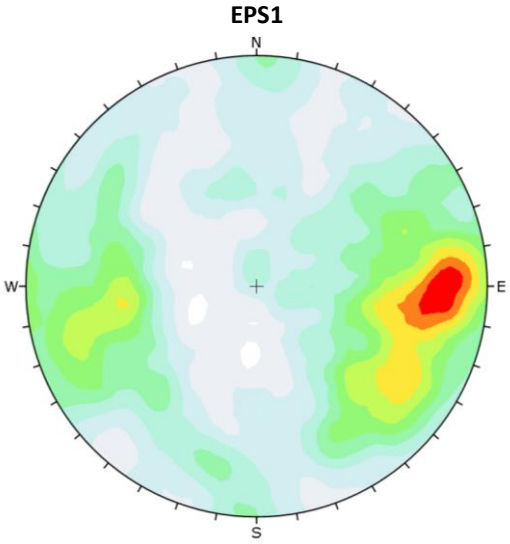

Figure 3. Isodensity (lower-hemisphere and equal angle) projection of poles of all fractures observed on core samples in EPS1 well drilled into Soultz-sous-Forêts geothermal site.

2.3 FRACTAL ANALYSIS OF 1D FRACTURE DATASETS

Two-point correlation functions of fracture intersection depths (in TVD except for RH-15) along each borehole were computed for 500 points logarithmically distributed uniformly in the range 0.1-10,000 *m.* The local slopes of the log-log plots of the *C(r)* function were computed for 25-point wide windows that were progressively moved across the *C(r)* curves without overlap. The correlation and slope functions of all fractures in the Basel-1, GPK1, GPK2, GPK3, GPK4 and RH-15 datasets are shown in Figures 4a-f respectively. Note that all fractures are included in the computation of correlation function regardless of their orientation.
The log-log slopes plots show a constant value for more than two orders of magnitude of *r*. The fractal dimensions are between 0.86-0.9 for all wells except RH-15. The associated errors are less than 0.06 for all cases except that of RH-15. A similar analysis was also performed on the fracture datasets from cores in EPS1 shown in Figure 5. The fractal dimension of the fracture patterns showed a value of 0.73 which is less than the fracture datasets from borehole images.

2.4 DEPTH-DEPENDENCE OF FRACTURE PATTERNS IN CRYSTALLINE ROCKS

The geometrical characteristics of fracture networks influences the hydraulic response of the system (Bonneau et al. 2016; Darcel et al. 2003a). Knowledge of the spatial distribution of the fractures along deep boreholes helps us to understand the structure of discontinuities in the crust. Ledésert et al. (1993) analyzed the fracture profiles derived from core samples from EPS1 and logs from GPK1 for the shallow (i.e. 1400-2200 m) reservoir at the Soultz-sous-Forêts site. They applied Cantor's Dust method (box-counting) to compute the fractal dimension of fracture spacing in windows taken along the boreholes and found evidence that fractal dimension increased with depth, which they proposed was related to the lithostatic pressure gradient. In contrast to Ledésert et al. (1993), here we applied the two-point correlation function method to

successive depth intervals taken along the Basel and Soultz boreholes to assess whether any systematic variation in fractal dimension of fracture spacing is resolved.

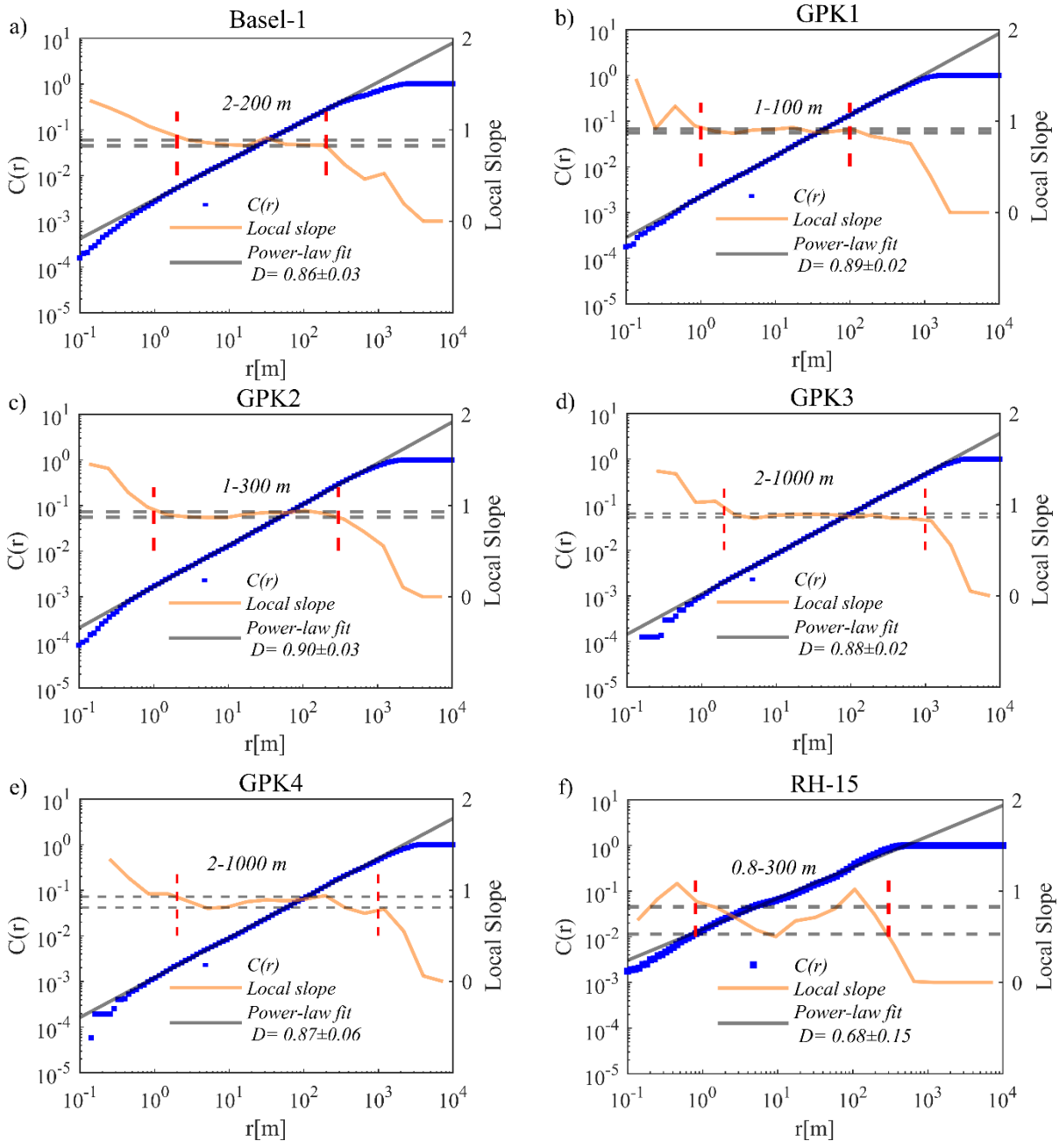

Figure 4. Correlation and log-log slope functions derived from all fractures intersecting (a) the Basel-1, (b) GPK1, (c) GPK2, (d) GPK3, (e) GPK4 and (f) RH-15 wells in the crystalline basement rock observed in borehole image logs. The study interval and the number of fractures are reported in Table 1. The dashed lines show the

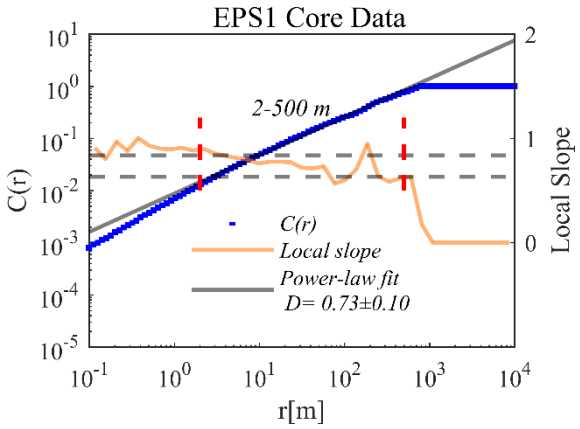

Figure 5. Correlation and log-log slope functions of fracture datasets from core samples in EPS1 well.

In each interval, two-point correlation functions were computed for 200 points uniformly spread logarithmically between 0.1 and 1000 m (i.e. 50 points per decade). The local slopes of the correlation functions were calculated by performing a linear fit over a 10-point wide window moved along the data with 75% overlap so as to give 20 slope values for every order of magnitude. Each log-log slope function was inspected to identify the range over which its value was reasonably constant, and a linear regression with a horizontal line performed to identify the correlation dimension and the standard deviation. In all cases, the plateau was seen to span at least 1.5 orders of magnitude in *r*. For all available datasets, 200 fractures were included in each window, and the latter moved along the profile in steps of 100 fractures, giving a 100 fracture overlap on successive windows so as to increase the number of D_{1D} determinations. Here, we analyzed five datasests that contain sufficient number of fractures for a extracting the profilde of fractal dimension versus depth. These datset are: 1) The fracture data from core samples in EPS1 and 2) The fracture data from image logs in Basel-1, GPK2, GPK3 and GPK4.

2.4.1 Core Dataset

The fracture density in 810 m cores from EPS1 borehole shows clusters of fractures indicating the fractured zones with higher densities as in Figure 6a. There are some shifts in the cumulative density plots in this interval but no systematic shifts in the cumulative fracture frequency is resolved (Figure 6b). The profile of *D* estimates are shown in Figure 6c together with the standard error from the linear regression. Evidently, no systematic change in *D* values is resolved, although the standard deviation estimates are large.

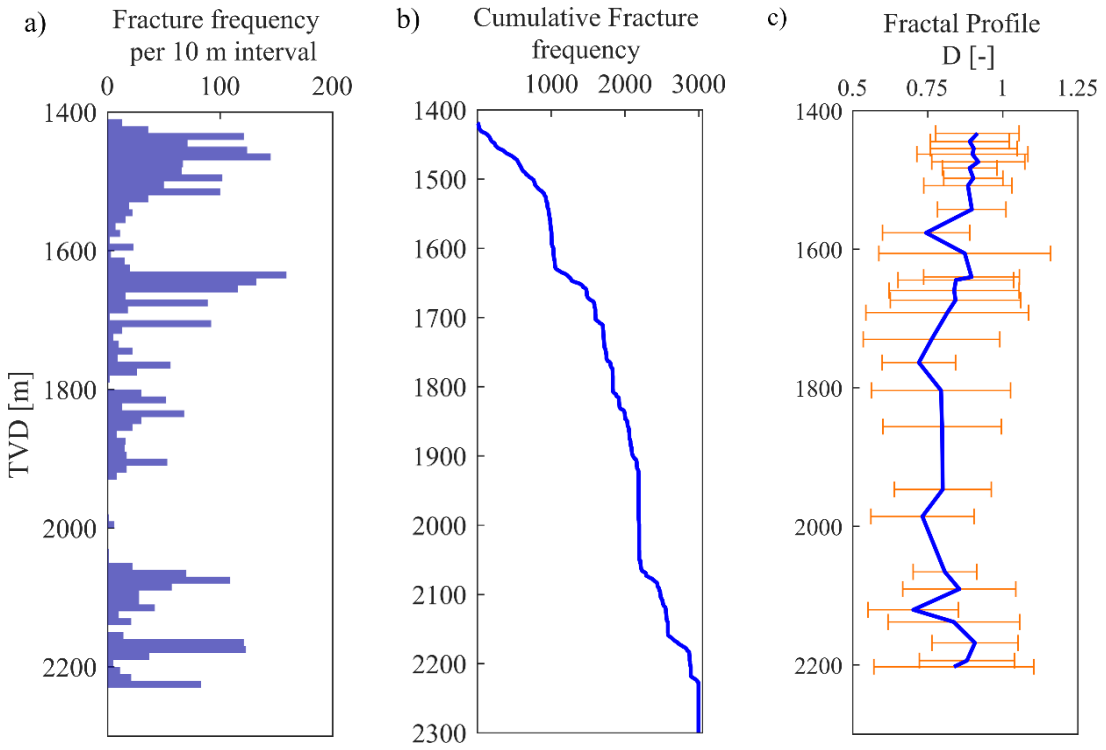

Figure 6. (a) Profile of the number of fractures per 10 m identified in the EPS-1 from cores (b) Profile of the cumulative number of fractures versus depth in the EPS-1 from cores (c) Variation of correlation dimension in moving windows containing 200 fractures with 100 overlaps in EPS-1. The estimates are drawn in the center of the data windows, and the error bars represent the standard deviation of the local slope within the fractal range.

2.4.2 Image Log Datasets

2.4.2.1 Basel-1

A complication of the Basel-1 dataset is posed by the higher fracture density seen at the top of the profile between 2600 and 3080 m, as shown in Figure 7a, which contains nearly 600 out of the total of 1164 fractures intersected by the well. It is obvious that the cumulative fracture density shows a shift at the depth of 3080 m, too (Figure 7b). This interval has been assumed to be the paleo-weathered surface . Because of the large number of fractures with shorter spacing, the plateau of the log-log slope function that denotes fractal scaling began for r as small as 0.1 m for intervals above $3080\ m$, whereas the start point was ~*1m* for intervals below. The profile of *D* estimates are shown in Figure 7c together with the standard error from the linear regression. Apparently, no systematic change in *D* values is resolved, although the standard deviation estimates are large.

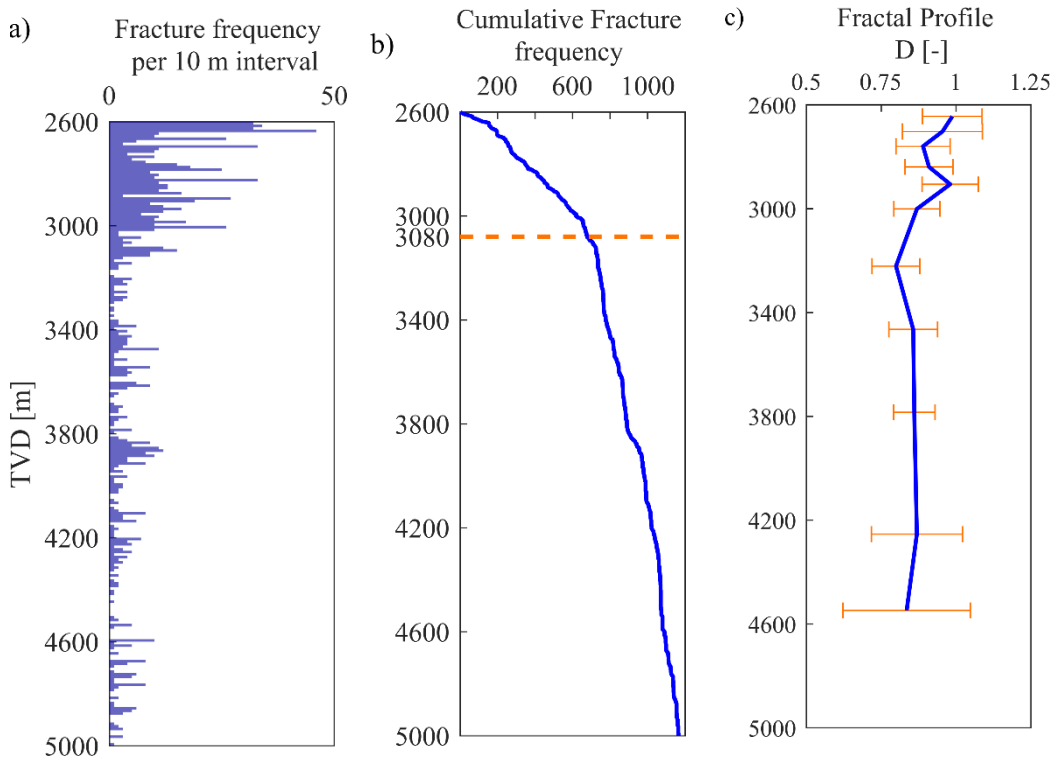

Figure 7. (a) Profile of the number of fractures per 10 m identified in the Basel-1 from image logs (b) Profile of the cumulative number of fractures versus depth in the Basel-1 from image logs (c) Variation of correlation dimension in moving windows containing 200 fractures with 100 overlaps in Basel-1. The estimates are drawn in the center of the data windows, and the error bars represent the standard deviation of the local slope within the fractal range.

2.4.2.2 GPK2

Similar analyses were performed on the GPK2 fracture dataset from Soultz-sous-Forêts using moving windows containing 200 fractures in steps of 100 fractures (i.e. 100 overlaps). Higher fracture density is observed at the top of the profile between 1400 and 2050 m, as shown in Figure 8a-b. A shift in the fracture density is also observed in a depth of 3250 m, too. This is may be related to the change of the lithological domains. The density change is very similar to the Basel-1 and the resulting fractal profiles shows higher fractal dimensions. However, no systematic varaiation of *D* is nor observed in Figure 8c.

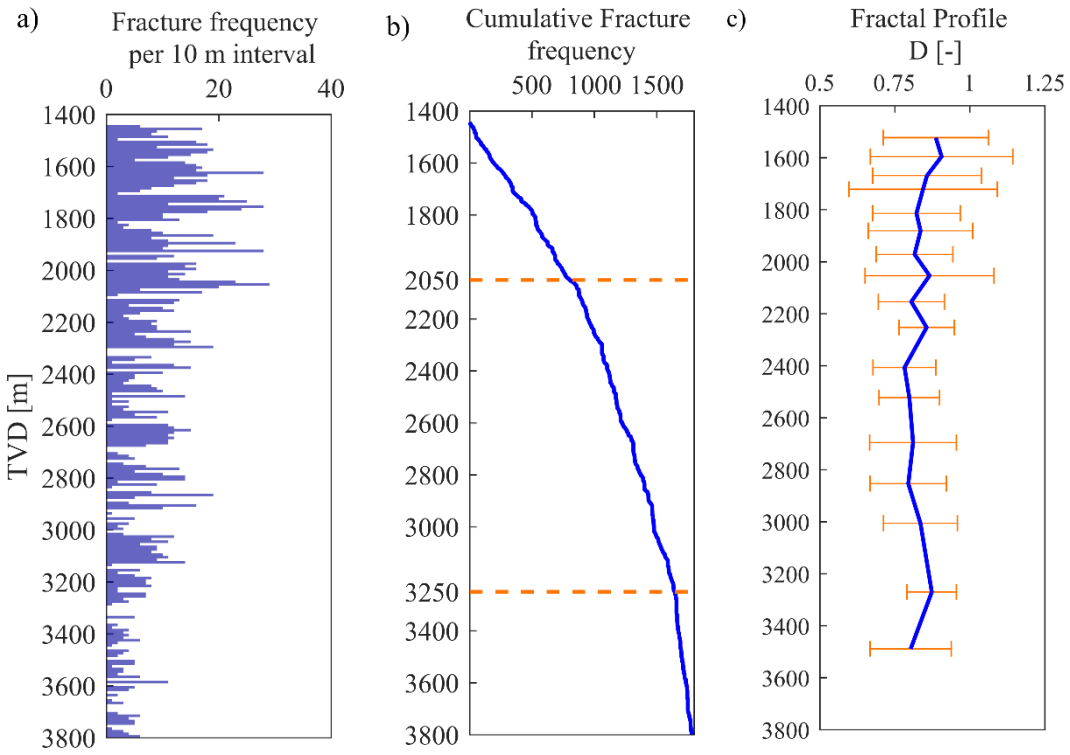

Figure 8. (a) Profile of the number of fractures per 10 m identified in the GPK2 from image logs (b) Profile of the cumulative number of fractures versus depth in the GPK2 from image logs (c) Variation of correlation dimension in moving windows containing 200 fractures with 100 overlaps in GPK2. The estimates are drawn in the center of the data windows, and the error bars represent the standard deviation of the local slope within the fractal range.

2.4.2.3 GPK3 and GPK4

Similar analyses were performed on the GPK3 and GPK4 fracture datasets from Soultz-sous-Forêts using moving windows containing 200 fractures in steps of 100 fractures (i.e. 100 overlaps), and the resulting profiles are shown in Figure 9a-c and Figure 10a-c respectively. The fracture density profiles of the wells shown in Figure 9a and Figure 10a, are more uniform than the Basel-1 and GPK2 case, and the plateau denoting the start of fractal scaling begins at a r value of $\sim 1\ m$. Similar to the case of Basel-1 and GPK2, there are some slight variations of the cumulative fracture denisty slopes versus depth. In GPK3, there are two variations in 2960 m and 4750 m. In addition, There are similar shifts in GPK4 in a depth of 3350 m and 4500 m. As in Basel-1 and GPK2, the lack of systematic depth variation in *D* is evident at the 1 sigma level, although the uncertainties are large.

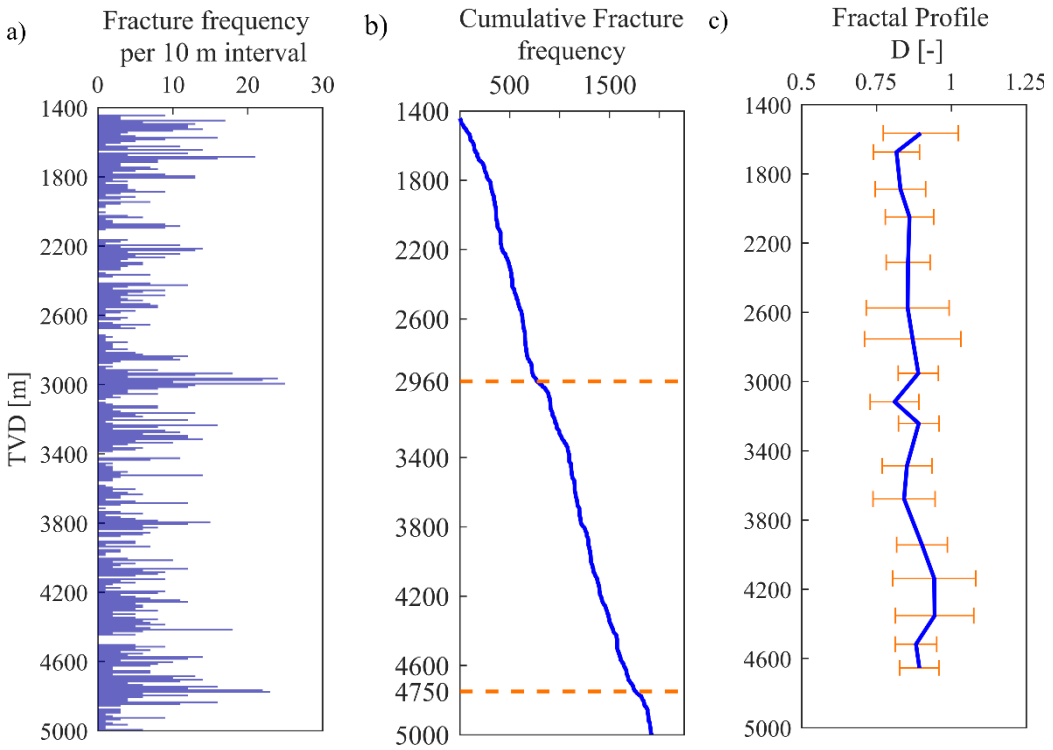

Figure 9. (a) Profile of the number of fractures per 10 m identified in the GPK3 from image logs (b) Profile of the cumulative number of fractures versus depth in the GPK3 from image logs (c) Variation of correlation dimension in moving windows containing 200 fractures with 100 overlaps in GPK3. The estimates are drawn in the center of the data windows, and the error bars represent the standard deviation of the local slope within the fractal range.

2.5 FRACTURE NETWORK MODEL

So far, we analyzed the 1D fracture datasets from deep boreholes and the fractal statistics of the spatial distribution of fractures. The fractal statistics are now used to derive synthetic 3D DFN models.

The dual power-law model (Davy et al. 1990) is a powerful mathematical representation of fractures that combines the spatial and size distribution of fractures in a 3D cubic volume in three dimensions of side length L following equation 3,

$$n(l,L)dl = \alpha . L^{D_{3D}} l^{-a_{3D}} dl, \quad l\epsilon[l_{min}, l_{max}] \qquad (3)$$

where $n(l,L)dl$ is the number of fractures having a length between l and $l+dl$, α is a constant of fracture density, D_{3D} is the correlation dimension of fracture centers in 3D space, and a is the length exponent (Davy et al. 1990). The dual power-law model has been widely used to study the hydromechanical properties of fractured rocks using fractal DFNs (Harthong et al. 2012; Lei and Gao 2018). Bour et al. (2002) have successfully validated this model by evaluating the scaling properties of multiscale fracture maps taken of outcrops in the Hornelen basin (Norway). A detailed step-by-step methodology to generate synthetic DFNs in 1D, 2D and 3D following equation 3 is presented in various research papers (e.g. Afshari Moein et al. 2019; Darcel et al.

2003b). Although the 3D DFNs were not initially planned in the objectives of the deliverable, the 3D models are highly desired to practical applications.

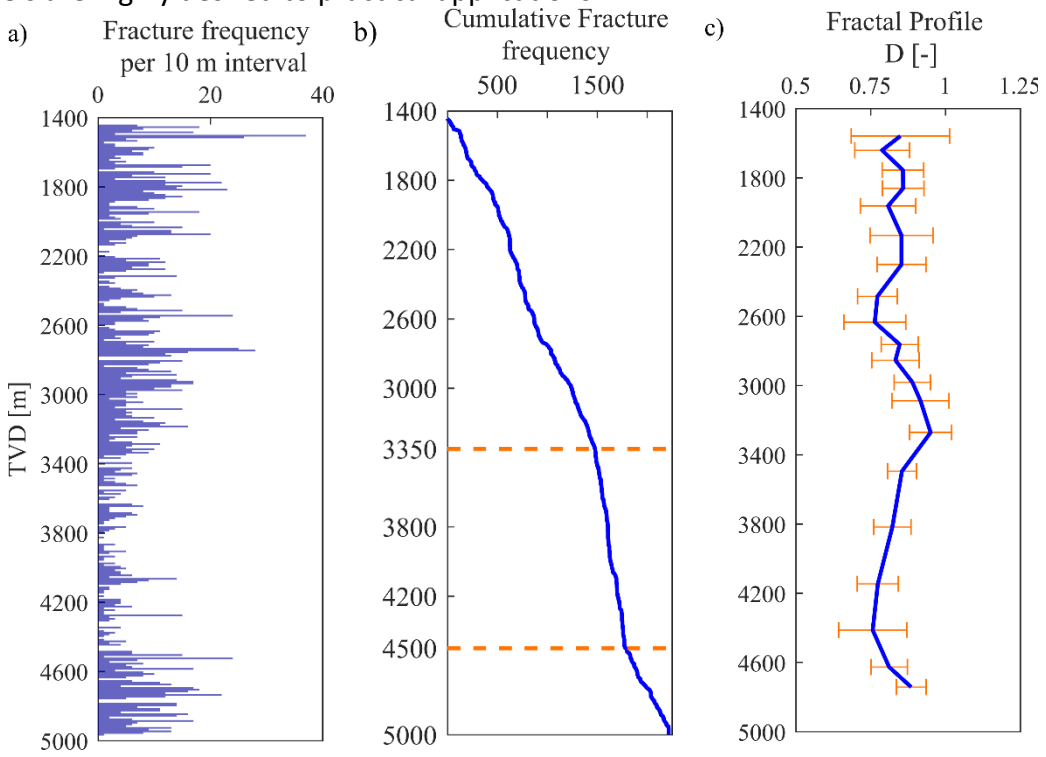

Figure 10. (a) Profile of the number of fractures per 10 m identified in the GPK4 from image logs (b) Profile of the cumulative number of fractures versus depth in the GPK4 from image logs (c) Variation of correlation dimension in moving windows containing 200 fractures with 100 overlaps in GPK4. The estimates are drawn in the center of the data windows, and the error bars represent the standard deviation of the local slope within the fractal range.

Figure 11 presents a 3D DFN model generated using the dual power-law model with the following parameters$D = 2.7$, $a = 2.8$ and $\alpha = 0.1$. One advantage of dual power-law models is the availability of valid stereological relationships for mapping from 1D to 3D. To our knowledge, the only model is a first-order fractal model of fracture length and density proposed by Davy et al. (2010). This model has successfully predicted maximum magnitude of induced seismicity in Basel based on clustering of size distribution of early microseismic events (Afshari Moein et al. 2018c). If equation 3 governs the spatial distribution of fracture centers and length distributions, we would be able to construct a three-dimensional probabilistic geological model from borehole observations, according to stereological relationships established by Darcel et al. (2003a). In the following chapter, such DFNs will be used with hydraulic modeling tools to study the circulation experiments in Soultz-sous-Forêts.

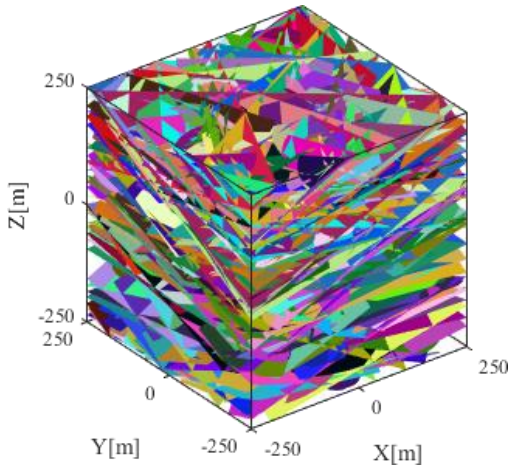

Figure 11. An example of a DFN model generated using dual power-law model with the $D = 2.7$, $a = 2.8$ and $\alpha = 0.1$.

2.6 MODELING HYDRAULIC CIRCULATION AT SOULTZ-SOUS-FORÊTS USING DFN MODELS

The circulation experiments coupled with a tracer test occurred between three wells by injecting at GPK3 and producing from GPK2 and GPK4 wells for five months in 2005. Discrete Fracture Networks (DFNs) are powerful tools to represent the heterogeneities of the rock mass at different scales to model the flow through the fractured rocks (Berkowitz 2002). Gentier et al. (2010) applied DFN models to simulate the 3D flow model of the circulation experiments at Soultz-sous-Forêts. The conceptual DFN was parameterized based on the fracture analyses from borehole images. Sanjuan et al. (2006) also analyzed the tracer tests in the circulation experiments and found a direct and fast connection between GPK2 and GPK3. However, they found a poor connection between GPK3 and GPK4. Among the previous studies, the mechanical effects not fully addressed.

Thus, we aim at developing a hydromechanical model of the circulation experiments. Here, a step-by-step methodology to generate a 3D hydromechanical model of the circulation experiments using a DFN approach is presented. However, this methodology is not fully implemented yet.

We will set up this model in Fracman software using the following steps:

1. Set-up a DFN model for Soultz based on the fracture network characterization from boreholes.
    - The analyses of the fracture patterns GPK2, GPK3 and GPK4 provides the fracture set characteristics. Then, the dual power-law model will be applied to generate fractal fracture patterns and parameterize it with the performed analyses in this deliverable. The 3D spatial distribution of fractures may be estimated from 1D fractal dimension, using the stereological relationships developed by Darcel et al. (2003c). The fracture length exponent may also be estimated from the rupture radius distribution of induced seismicity (Afshari Moein et al. 2018a). The number of fractures also may be constrained using borehole data.

- All statistical parameters of the DFNs should be derived from the borehole data and induced seismicity pattern. The DFN will be generated using the dual power-law model and imported to Fracman.
- Run critical stress analysis using the geomechanical module of Fracman. Apply the stress field estimates in the given depth at Soultz provided by Valley and Evans (2007).

2. Explore the slip and/or dilation tendency of the fractures.
3. Run hydraulic circulation experiments with the hydraulic module of Fracman
   - Compare the breakthrough curves with that of the modeled DFNs.
4. Run hydromechanical analysis
   - The purpose is to see the effect of mechanical properties (i.e. reduced shear) of the rock mass on the hydraulic response in a coupled simulation.
5. Derive induced seismicity patterns and compare with seismic catalogues.
6. If the DFNs do not provide similar breakthrough curves, include the seismicity data points into the initial DFN in step 2 and repeat the step 3-7.

2.7 DISCUSSION AND OUTLOOK

Setting up Discrete Fracture Network models conditioned to the data from boreholes or outcrops are essential to subsurface rock mass characterization programs including EGS developments (e.g. Watanabe and Takahashi 1993). The computation of 1D correlation dimension for the fracture datasets from cores and borehole images of seven deep boreholes showed that fracture populations follow fractal statistics in more than two orders of magnitude. The fractal analyses of fracture datasets from one deep borehole in Basel, Switzerland (Basel-1) and four deep boreholes in Soultz-sous-Forêts, France (GPK1, GPK2, GPK3 and GPK4) leads to very similar values ranging from 0.86 to 0.9. Such a similarity may be justified by the same tectonic settings (i.e. the Upper Rhine Graben system) that all the five wells were located. In that regard, the data from the boreholes GPK2, GPK3 and GPK4 are of particular interest because in the upper kilometer of the granite section the distance between the boreholes is less than 30 m and they sample essentially the same rock mass volume. The inter-well distance increases up to 700 m toward the bottom of the boreholes. Thus, the persistance of the correlation dimension in these boreholes indicate not only a depth homogeneity of the fracturing fractal characteristics, but although a lateral homogeneity within the sampled volume between the boreholes. However, the fractal dimension of fractures in RH-15 was slightly less (0.68). This may indicate different geological setting and lithologies in Rosemanowes geothermal project. Furthermore, the fractal dimension of the fractures from core samples in EPS1 is 0.73 indicating more clustered fracture patterns. The difference between scaling exponent of fractures from cores and image logs originates from the limited resolution of borehole imagery. Genter et al. (1997) performed a comparative study of the fracture datasets from cores and image logs. They concluded that image logs can only detect 20% of the fractures that are detected by cores. This imposes a large uncertainty on fracture network characterization from image logs. Note that the number of fractures strongly influences the fractal dimension estimations. Despite these limitations, the scaling parameters are valid over more than two orders of magnitudes, i.e. typically in the range 2 to 200 m. This constitutes a strong evidence and support that the fracture networks investigated in granitic rocks follow a fractal organization.

The detailed analyses of the fracture patterns in Basel-1, GPK2, GPK3 and GPK4 showed variations of fracture frequency with depth. However, no systematic trend is observed. No clear trend of fractal dimension is resolved in any of the data examined neither from cores nor image logs. The depth-dependence analyses of the fractures in deep boreholes indicate that a unique fractal model, such as dual power-law model, may be implemented to represent the fracture population in a rock mass. However, the change in the fracture frequency must be considered by changing the fracture density or intensity parameters. For the case of dual power-law model, the parameter of α must be adjusted. Furthermore, fracture intensity for 3D networks may be defined as ratio of the total fracture area to the domain volume (P_{32}).

In this deliverable, we performed a fundamental analysis on the scaling properties of fractures in deep borehole. This is the necessary step toward modelling the fluid flow in fractured rocks. However, the circulation models are not fully developed, yet. This deliverable reported the latest progress on developing a methodology to set up a hydromechanical model of the circulation experiments at Soultz-sous-Forêts.

2.8 REFERENCES

Afshari Moein M, Valley B, Tormann T, Wiemer S Relation between Induced Microseismicity and Fracture Network in the Basel Geothermal Site. In: 80th EAGE Conference and Exhibition 2018, 2018a.

Afshari Moein MJ, Somogyvári M, Valley B, Jalali M, Loew S, Bayer P (2018b) Fracture Network Characterization Using Stress-Based Tomography J Geophys Res-Sol Ea 123:9324-9340 doi:10.1029/2018jb016438

Afshari Moein MJ, Tormann T, Valley B, Wiemer S (2018c) Maximum Magnitude Forecast in Hydraulic Stimulation Based on Clustering and Size Distribution of Early Microseismicity Geophysical Research Letters 45:6907-6917 doi:10.1029/2018gl077609

Afshari Moein MJ, Valley B, Evans KF (2019) Scaling of Fracture Patterns in Three Deep Boreholes and Implications for Constraining Fractal Discrete Fracture Network Models Rock Mechanics and Rock Engineering doi:10.1007/s00603-019-1739-7

Allegre CJ, Lemouel JL, Provost A (1982) Scaling Rules in Rock Fracture and Possible Implications for Earthquake Prediction Nature 297:47-49 doi:DOI 10.1038/297047a0

Barton CA, Zoback MD (1992) Self-similar distribution and properties of macroscopic fractures at depth in crystalline rock in the Cajon Pass Scientific Drill Hole Journal of Geophysical Research: Solid Earth (1978–2012) 97:5181-5200

Berkowitz B (2002) Characterizing flow and transport in fractured geological media: A review Advances in Water Resources 25:861-884 doi:http://dx.doi.org/10.1016/S0309-1708(02)00042-8

Berkowitz B, Hadad A (1997) Fractal and multifractal measures of natural and synthetic fracture networks Journal of Geophysical Research-Solid Earth 102:12205-12218 doi:Doi 10.1029/97jb00304

Boadu F, Long L The fractal character of fracture spacing and RQD. In: International journal of rock mechanics and mining sciences & geomechanics abstracts, 1994. vol 2. Elsevier, pp 127-134

Bonneau F, Caumon G, Renard P (2016) Impact of a stochastic sequential initiation of fractures on the spatial correlations and connectivity of discrete fracture networks J Geophys Res-Sol Ea 121:5641-5658

Bonnet E, Bour O, Odling NE, Davy P, Main I, Cowie P, Berkowitz B (2001) Scaling of fracture systems in geological media Reviews of Geophysics 39:347-383 doi:10.1029/1999RG000074

Bour O, Davy P, Darcel C, Odling N (2002) A statistical scaling model for fracture network geometry, with validation on a multiscale mapping of a joint network (Hornelen Basin, Norway) J Geophys Res-Sol Ea 107

Chilès J (1988) Fractal and geostatistical methods for modeling of a fracture network Mathematical Geology 20:631-654

Darcel, Bour O, Davy P, De Dreuzy J (2003a) Connectivity properties of two-dimensional fracture networks with stochastic fractal correlation Water resources research 39

Darcel, Bour O, Davy P, de Dreuzy JR (2003b) Connectivity properties of two-dimensional fracture networks with stochastic fractal correlation Water Resources Research 39:n/a-n/a doi:10.1029/2002WR001628

Darcel C, Bour O, Davy P (2003c) Stereological analysis of fractal fracture networks J Geophys Res-Sol Ea 108

Davy P, Sornette A, Sornette D (1990) Some consequences of a proposed fractal nature of continental faulting Nature 348:56-58

Dezayes C, Genter A, Hooijkaas GR Deep-seated geology and fracture system of the EGS Soultz reservoir (France) based on recent 5km depth boreholes. In: Proceedings World Geothermal Congress, 2005.

Dezayes C, Genter A, Valley B (2010) Structure of the low permeable naturally fractured geothermal reservoir at Soultz Comptes Rendus Geoscience 342:517-530 doi:https://doi.org/10.1016/j.crte.2009.10.002

Edwards B, Kraft T, Cauzzi C, Kästli P, Wiemer S (2015) Seismic monitoring and analysis of deep geothermal projects in St Gallen and Basel, Switzerland Geophysical Journal International 201:1022-1039

Ehlen J (2000) Fractal analysis of joint patterns in granite International Journal of Rock Mechanics and Mining Sciences 37:909-922 doi:https://doi.org/10.1016/S1365-1609(00)00027-7

Evans, Zappone A, Kraft T, Deichmann N, Moia F (2012) A survey of the induced seismic responses to fluid injection in geothermal and CO2 reservoirs in Europe Geothermics 41:30-54

Evans KF (2005) Permeability creation and damage due to massive fluid injections into granite at 3.5 km at Soultz: 2. Critical stress and fracture strength J Geophys Res-Sol Ea 110

Evans KF, Genter A, Sausse J (2005) Permeability creation and damage due to massive fluid injections into granite at 3.5 km at Soultz: 1. Borehole observations J Geophys Res-Sol Ea 110

Genter A, Castaing C, Dezayes C, Tenzer H, Traineau H, Villemin T (1997) Comparative analysis of direct (core) and indirect (borehole imaging tools) collection of fracture data in the Hot Dry Rock Soultz reservoir (France) Journal of Geophysical Research: Solid Earth (1978–2012) 102:15419-15431

Genter A, Evans K, Cuenot N, Fritsch D, Sanjuan B (2010) Contribution of the exploration of deep crystalline fractured reservoir of Soultz to the knowledge of enhanced geothermal systems (EGS) Comptes Rendus Geoscience 342:502-516 doi:http://dx.doi.org/10.1016/j.crte.2010.01.006

Genter A, Traineau H (1992) Borehole EPS-1, Alsace, France: preliminary geological results from granite core analyses for Hot Dry Rock research Scientific Drilling 3:205-214

Genter A, Traineau H, Dezayes C, Elsass P, Ledésert B, Meunier A, Villemin T Fracture analysis and reservoir characterization of the granitic basement in the HDR Soultz project (France). In: International journal of rock mechanics and mining sciences & geomechanics abstracts, 1996. vol 2. Elsevier Science, pp 69A-69A

Gentier S, Rachez X, Ngoc TDT, Peter-Borie M, Souque C 3D flow modelling of the medium-term circulation test performed in the deep geothermal site of Soultz-sous-Forêts (France). In: World Geothermal Congress 2010, 2010. p 13 p.

Häring MO, Schanz U, Ladner F, Dyer BC (2008) Characterisation of the Basel 1 enhanced geothermal system Geothermics 37:469-495

Harthong B, Scholtès L, Donzé F-V (2012) Strength characterization of rock masses, using a coupled DEM–DFN model Geophysical Journal International 191:467-480

Hentschel HGE, Procaccia I (1983) The infinite number of generalized dimensions of fractals and strange attractors Physica D: Nonlinear Phenomena 8:435-444 doi:https://doi.org/10.1016/0167-2789(83)90235-X

Hirata T, Satoh T, Ito K (1987) Fractal structure of spatial distribution of microfracturing in rock Geophysical Journal International 90:369-374 doi:10.1111/j.1365-246X.1987.tb00732.x

La Pointe P A method to characterize fracture density and connectivity through fractal geometry. In: International Journal of Rock Mechanics and Mining Sciences & Geomechanics Abstracts, 1988. vol 6. Elsevier, pp 421-429

Ledésert B, Dubois J, Genter A, Meunier A (1993) Fractal analysis of fractures applied to Soultz-sous-Forêts hot dry rock geothermal program Journal of Volcanology and Geothermal Research 57:1-17

Lei Q, Gao K (2018) Correlation between Fracture Network Properties and Stress Variability in Geological Media Geophysical Research Letters

Lei Q, Latham J-P, Tsang C-F (2017) The use of discrete fracture networks for modelling coupled geomechanical and hydrological behaviour of fractured rocks Computers and Geotechnics 85:151-176

Lei Q, Wang X (2016) Tectonic interpretation of the connectivity of a multiscale fracture system in limestone Geophysical Research Letters 43:1551-1558

Moeck I et al. The St. Gallen project: development of fault controlled geothermal systems in urban areas. In: Proceedings World Geothermal Congress, 2015.

Moein M, Valley B, Ziegler M (2016) Preliminary fractal analysis of fracture spacing inferred from an acoustic televiewer log run in the Basel-1 geothermal well (Switzerland). In: Rock Mechanics and Rock Engineering: From the Past to the Future. CRC Press, pp 1103-1107

Odling (1992) Network properties of a two-dimensional natural fracture pattern Pure and Applied Geophysics 138:95-114

Sanjuan B et al. (2006) Tracer testing of the geothermal heat exchanger at Soultz-sous-Forêts (France) between 2000 and 2005 Geothermics 35:622-653

Sausse J, Dezayes C, Genter A, Bisset A Characterization of fracture connectivity and fluid flow pathways derived from geological interpretation and 3D modelling of the deep seated EGS reservoir of Soultz (France). In: Proceedings, thirty-third workshop on Geothermal Reservoir Engineering, Stanford, California, 2008.

Somogyvári M, Jalali M, Jimenez Parras S, Bayer P (2017) Synthetic fracture network characterization with transdimensional inversion Water Resources Research 53:5104-5123

Tester JW et al. (2006) The future of geothermal energy: Impact of enhanced geothermal systems (EGS) on the United States in the 21st century Massachusetts Institute of Technology 209

Tezuka K, Watanabe K Fracture network modeling of Hijiori hot dry rock reservoir by deterministic and stochastic crack network simulator (D/SC). In: Proceeding World Geothermal Congress 2000, 2000.

Torabi A, Berg SS (2011) Scaling of fault attributes: A review Marine and Petroleum Geology 28:1444-1460

Valley, Evans KF Stress state at Soultz-sous-Forêts to 5 km depth from wellbore failure and hydraulic observations. In: Proceedings, 32nd Workshop on Geothermal Reservoir Engineering, 2007. pp 17481-17469

Valley B, Evans K (2015) Methods for characterizing deep geothermal reservoirs from borehole measurements. In: Hirschberg S, Wiemer S, Burgherr P (eds) Energy from the Earth. vdf Hochschulverlag, pp 64-81

Valley BıC (2007) The relation between natural fracturing and stress heterogeneities in deep-seated crystalline rocks at Soultz-sous-Forêts (France). Université de Neuchâtel, Switzerland

Velde B, Dubois J, Touchard G, Badri A (1990) Fractal analysis of fractures in rocks: the Cantor's Dust method Tectonophysics 179:345-352

Watanabe K, Takahashi H Fractal characterization of subsurface fracture network for geothermal energy extraction system. In: Proceedings, eighteent workshop on geothermal reservoir engineering, Stanford University, Stanford, CA. Report No. SGP-TR-145-17, 1993.

Ziegler M, Valley B, Evans KF Characterisation of natural fractures and fracture zones of the Basel EGS reservoir inferred from geophysical logging of the Basel-1 well. In: World Geothermal Congress Melbourne, Australia, 2015. pp 19-25